EXPLORATORY SUBSONIC INVESTIGATION OF VORTEX-FLAP CONCEPT ON ARROW WING CONFIGURATION*

Dhanvada M. Rao
Old Dominion University Research Foundation

SUMMARY

The drag-reduction potential of a vortex-flap concept, utilizing the thrust contribution of separation vortices maintained over leading-edge flap surfaces, has been explored in subsonic wind tunnel tests on a highly swept arrow wing configuration. Several flap geometries were tested in comparison with a previous study on the same model with leading edges drooped for attached flow. The most promising vortex-flap arrangements produced drag reductions comparable with leading-edge droop over a range of lift coefficients from 0.3 to 0.6 (untrimmed), and also indicated beneficial effects in the longitudinal and lateral static stability characteristics.

INTRODUCTION

The low-speed aerodynamics of highly swept, slender wings favored for supersonic cruise aircraft continues to receive attention on account of its serious performance, stability and control deficiencies. Leading-edge flow separation and resulting vortices are known to be the primary cause of drag and longitudinal instability problems encountered on such configurations at angles of attack. Control of separation at highly swept leading edges therefore has attracted much interest and remains a research and engineering problem with high pay-off potential.

An obvious approach to the problem is the use of leading-edge droop, which past experience has shown to be an effective means to raise the angle of attack limit for attached flow and thus delay the drag increase to a higher lift coefficient. It has limitations however on highly swept wings (leading-edge sweep of 70° or greater) where the circulation-induced upwash normal to the leading edges grows rapidly not only with angle of attack but also in a spanwise direction. A highly warped leading edge with pronounced droop angles will therefore be needed for fully attached flow subsonically. Since the drag penalty of such a leading edge could not be tolerated in supersonic cruise, an articulated and

* Research Supported by NASA Grant no. NSG-1315

mechanically complex leading-edge design with associated weight penalties appears inevitable. Also, the possibility of separation inboard along the highly curved knee-line (fig. 1, C) may limit the advantage of attached leading-edge flow. While the aerodynamic potential of optimally tailored droop on highly swept wings has been demonstrated (ref. 1), the question remains as to the feasibility of its realization in practice.

The vortex-flap concept is an alternative approach to swept leading-edge flow management with a view to retain effective leading-edge suction beyond the normal attached-flow angle of attack regime. It is based on controlle' separation to produce coiled vortices whose suction effect over inclined leading-edge surfaces is utilized to generate a thrust component. Although unconventional, this approach is based on flow mechanisms that are physically well understood viz. streamwise vortices arising from swept-edge separations and their powerful interaction with the inviscid flow field.

The vortex-flap device is conceived here as a surface hinged just under the leading edge and retracted flush with the wing undersurface when inoperative (fig. 1, D). To deploy the flap, it is rotated forward and set at an angle less than the local upwash, forcing separation and a resultant coiled vortex close to its upper surface. The high degree of leading-edge sweep promotes stability and persistence of the vortex down the length of the flap. For most efficient utilization of the flap surface under the vortex suction and also for smooth entry to the wing, the vortex-induced reattachment should occur just at the wing leading edge as indicated in figure 1, D.

Proof-of concept tests were conducted at NASA Langley on a 74^{o} delta wing research model for an initial assessment of the vortex-flap potential and to obtain a general understanding of the flap geometry variables of importance (ref. 2). The results of these trials were sufficiently encouraging to prompt further studies using a supersonic cruise configuration on which an extensive data base already existed, particularly with regard to leading-edge droop effects. Selected results of these exploratory investigations are presented in this paper to provide an indication of the drag-reduction potential of the vortex-flap concept relative to drooped leading edges and its impact on other low-speed aerodynamic characteristics of a realistic airplane configuration.

SYMBOLS

C_L	lift coefficient
C_D	drag coefficient
C_m	pitching moment coefficient
L/D	lift-to-drag ratio
α	angle of attack (deg.)

SYMBOLS (concluded)

β angle of sideslip (deg.)

C_{n_β} body-axis directional static stability de ivative (per deg.)

C_{l_β} body-axis lateral static stability derivative (per deg.)

PRELIMINARY VORTEX-FLAP EXPERIMENTS ON A DELTA WING

The initial trials of the leading edge vortex-flap (LEVF) concept were conducted on a flat-plate type 74° delta wing model with leading edges modified to a constant radius semi-circular section, in the NASA Langley 7x10 ft. high speed tunnel at a nominal Mach number of 0.2 (Reynolds number = 2.7×10^6 based on mean aerodynamic chord). The details of this test program and the results are reported in reference 2. A series of systematically-varied LEVF geometries were investigated, including constant chord full-length and part-length flaps and inverse-taper flaps, at two deflection angles (30° and 45° normal to the leading edge). The flap area was progressively reduced from over 25% to about 15% of the basic wing area through successive geometric refinements for improving the drag-reduction effectiveness.

A typical set of data pertaining to the final LEVF configuration of this test series is presented in figure 2. Also shown for comparison are the sharp leading edge data previously obtained on the same wing (see NASA TN D-6344) which correspond to zero leading-edge suction, as well as a calculated 100% suction curve for the blunt leading edge. These comparisons serve to indicate the lift/drag ratio benefits obtained largely as a result of lift-dependent drag reductions relative to the basic wing. A small part of the indicated improvement is due to the extra lift from the planform area addition of the flaps, which of course is integral to the present LEVF concept. It is noteworthy that the beneficial effect of LEVF is sustained to the highest lift coefficient (1.0) of the test range. The pitching moment characteristics with LEVF also shown in figure 2 remain linear in the C_L range of interest with only a small reduction in pitch stability.

VORTEX-FLAP STUDIES ON SWAT CONFIGURATION

As part of a research program aimed at advancing the subsonic limitations in swept wing aerodynamic technology (SWAT), the potential of leading-edge droop has been the subject of recent wind tunnel investigations at Langley on an arrow wing supersonic cruise aircraft configuration. The SWAT model details and analysis of data are presented in reference 1. These data were used to provide a reference for assessing LEVF arrangements studied in follow-on tests with the

same model in the Langley 7x10 ft. high speed tunnel. Selected results from these tests are presented and discussed below (test conditions: Mach no. = 0.14, Reynolds no. = 2.8×10^6 based on mean aerodynamic chord).

Vortex-Flap Details

The two final LEVF geometries of the present test series are shown in figure 3. The segmented arrangement of these LEVF designs distinguishes them from the one-piece flaps earlier tested on the 74° delta wing research model. At least two flap-segments (LEVF #9) were necessitated because of a break in the leading-edge sweep angle at about 50% semi-span location on the present configuration. A four-segment variation (LEVF #8) was also tested for a first look at multi-segment LEVF arrangements which permit spanwise tailoring of deflection angle to maximize drag-reduction and possibly for some pitching-moment control for trim; they may also be considered more practical than one-piece flaps on large vehicles. The limited scope of this study however covered only one deflection schedule for each LEVF arrangement as indicated in figure 3 (note that the tip panel leading-edge flap was always deflected down 50° unless otherwise stated, as this was found beneficial for drag at the higher angles of attack).

The total area of the four-segment flap arrangement was about two-thirds the two-segment LEVF and amounted to 10.5% of the wing reference area. The maximum flap chord (normal to hinge line) was 7.5% of the mean aerodynamic chord in both the LEVF configurations. The flap elements were cut from 1.6 mm thick aluminum sheet, bent as required and secured with screws under the leading edges which were in the undrooped position. No attempt was made to fair-in the steps and other protrusions resulting from this somewhat crude attachment method, and it is probably fair to assume that the LEVF installation drag was relatively much more on the wind tunnel model than will be incurred on a flight vehicle.

Lift and Drag Characteristics

The lift and drag measurements with LEVF (symbols) are compared with the data of reference 1 (curves) in figure 4. In addition to undrooped leading edge, data for two leading-edge droop configurations are available, one with constant 30° droop and the other with droop angle increasing continuously from 16° at the fuselage junction to 50° at the tip. The effectiveness of droop may be judged by the elimination of a distinctive upward break in the lift-curve slope found on the undrooped wing. However, elimination of vortices results in a lift loss of as much as 17% at 8° angle of attack. The lift data with LEVF arrangements are practically linear in the angle of attack range and indicate a much smaller lift loss.

The drag data (plotted versus C_L^2) in figure 4 show that LEVF #9 equals the drag-reduction capability of the 16°-50° droop configuration which probably represents the best attached-flow performance. The four-segment flap (LEVF #8) with 30% less flap area comes quite close to the performance of LEVF #9. These trends are further illustrated in terms of lift-to-drag ratio in figure 5.

The above LEVF data correspond to the tip panel leading-edge flap at 50°. Comparison with data for undeflected leading edge (figure 6 shows that a significant L/D gain results from this relatively simple tip-panel leading edge device. Although they have only 7.5% of the total wing area, the tip panels comprise 30% of the exposed span and therefore the effect of loss of leading-edge suction at the tip panels is substantial. The wing tips evidently operate in a region of high induced upwash even at moderate lift coefficients and so are prone to early stall. The data of figure 6 are indicative of the importance of flow management in this area not only for drag minimization, but also with regard to longitudinal stability as will be found in the following section.

Longitudinal Stability

The pitching moment characteristics with LEVF are compared with the results from reference 1 in figure 7 (note that these data pertain to 'tail off' condition since the aft fuselage and the empennage were not represented on the SWAT model). The undrooped leading edge data indicate a pitch-up at about $C_L = 0.35$, which could be caused by wing leading-edge separation or tip-panel stall, or both. With droop, this adverse feature is moderated. The pitching moment measurements with LEVF (taken about the same center-of-gravity position and therefore showing a positive slope) are linear up to $C_L = 0.45$ before a pitch-up appears; however the relative change of the moment-curve slope at pitch-up is only 20% of that on the undrooped wing, representing a considerable alleviation of the pitch-up intensity.

Additional tests with the tip panels removed were carried out in an attempt to separate out the tip-panel stall and leading-edge separation effects on the pitch-up behavior. With undrooped leading edge the data show that removing the tip panels does not essentially alter the pitch-up angle of attack, but the pitch-up intensity is much reduced (fig. 8). This result would indicate that leading-edge separation and tip stall both take place at the same time producing the strong pitch-up found with undrooped leading edges. With 30° droop and tip panels off the pitch-up is eliminated.

The LEVF effect on pitching moment without the tip panels is shown in figure 9. Not only is the pitch-up delayed to about 8° angle of attack but also the pitch-up intensity is much softened. It would appear that the vortex-flaps act partly as droop in alleviating the vortex strength over the wing.

Lateral/Directional Stability

The tail-off directional and lateral static stability derivatives for LEVF #8 obtained from tests at $\pm 5^{o}$ sideslip angle are compared with the undrooped and 30^{o} droop data in figure 10. A rapid rise in directional stability of the undrooped wing starting at a lift coefficient corresponding to vortex onset suggests that it is related to the favorable asymmetry in the vortex pair found on slender lifting bodies of oblate cross-sections at sideslip, which generate upwind suction and corresponding restoring yawing moments (ref. 3). This feature is notably absent in the directional data for 30^{o} droop where the vortices have been suppressed, and also with LEVF. This loss of vortex-related directional stability is not necessarily a bad feature since restoring side-forces that originate forward of the center-of-gravity also reduce yaw damping; it is therefore preferable to seek directional stability by the use of conventional aft vertical surfaces.

The combined effect of high sweep angle and low aspect ratio is to produce a high level of lateral static stability on the present arrow-wing configuration, as indicated by the data for undrooped leading edges in figure 10. Leading-edge droop does little to change this feature in the C_L range of interest. Because of limited roll control capability typical of such configurations, the high lateral stability compromises cross-wind approach and landing operations. In this context, the lateral derivative data with LEVF shown in figure 10 are of particular interest. They indicate a 20% lower dC_{l_β}/dC_L compared to the undrooped wing, resulting in a 25% reduction in C_{l_β} at a lift coefficient of 0.4. If this were a straight-forward anhedral effect, a change in the gradient dC_{l_β}/dC_L would not be expected. The ΔC_{l_β} due to vortex-flap in this instance is of the same order as demonstrated in reference 1 by the use of geometric anhedral on the same model; however the degree of anhedral needed may exceed the tip clearance constraints with a normal landing gear length. This favorable LEVF effect on lateral stability indicated by the present limited data appears sufficiently promising to merit further investigation.

Flow Visualization

Smoke visualization experiments were conducted at a very low speed (about 3 m/sec.) in an attempt to observe the qualitative nature of the flow over leading edge vortex-flaps. A thin plane of light illuminated a chosen cross-flow section of the model. A smoke-generating wand was held upstream of the model while photographs of the smoke pattern were taken from a downstream position at various angles of attack. The light plane was moved to different areas of the flaps to observe the origin and development of the vortices. At angles of attack of about 10^{o} and greater, well-defined vortex cores could be seen over the flap segments. A typical visualization photograph is presented in figure 11.

CONCLUSIONS

The potential of leading edge vortex-flaps (LEVF) in reducing the subsonic lift-dependent drag of a representative supersonic cruise aircraft configuration was explored through wind tunnel tests. Two different LEVF arrrangements (a two-segment and a four-segment) were assessed by comparison with results from a previous test on the same model with the leading edges drooped for attached flow. The main results of this study may be summarized as follows:

1. The two-segment vortex-flaps (14.8% of the wing area) produced drag reductions equal to that obtained by optimally drooped leading edges at lift coefficients greater than 0.4.

2. The four-segment vortex-flaps (10.5% of wing area) performed as well as the constant 30^{o} droop configuration.

3. The vortex-flaps raised the pitch-up angle of attack from 5^{o} to 8^{o} and also allayed its severity.

4. The vortex-flaps had the same effect as leading-edge droop in eliminating the vortex-related directional stability at higher angles of attack.

5. A 20% reduction in lateral stability was achieved at lift coefficients up to 0.5, indicating that vortex-flaps can contribute significantly towards improving cross-wind landing performance in addition to reducing drag.

REFERENCES

1. Coe, Paul L., Jr. and Huffman, Jarrett K.: Influence of Optimized Leading-Edge Deflection and Geometric Anhedral on the Low-Speed Aerodynamic Characteristics of a Low-Aspect-Ratio Highly Swept Arrow-Wing Configuration. NASA TM 80083, 1979.

2. Rao, Dhanvada M.: Leading Edge Vortex-Flap Experiments on a 74^{o} Delta Wing. NASA CR-159161, 1979.

3. Chambers, Joseph R.; Gilbert, William P. and Grafton, Sue B.: Results of Recent NASA Studies on Spin Resistance. Paper no. 6, AGARD CP-199, 1975.

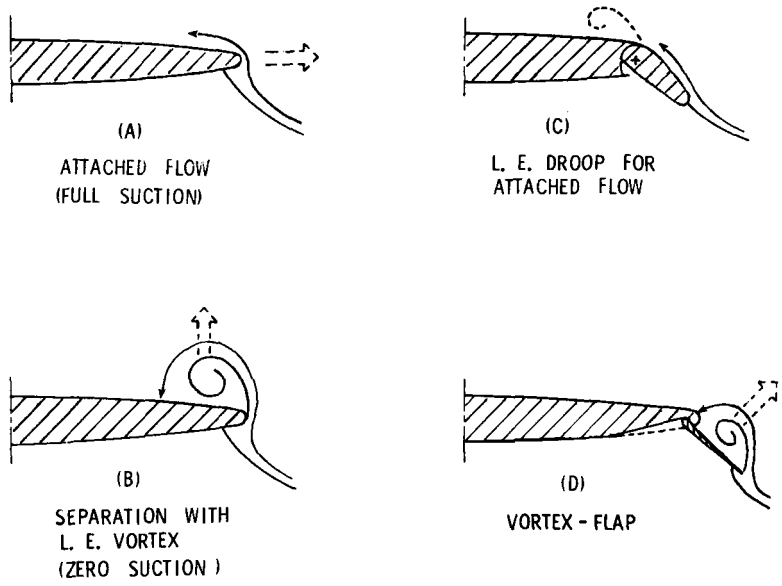

Figure 1.- Leading-edge flows over highly swept wing (viewed in cross-flow plane).

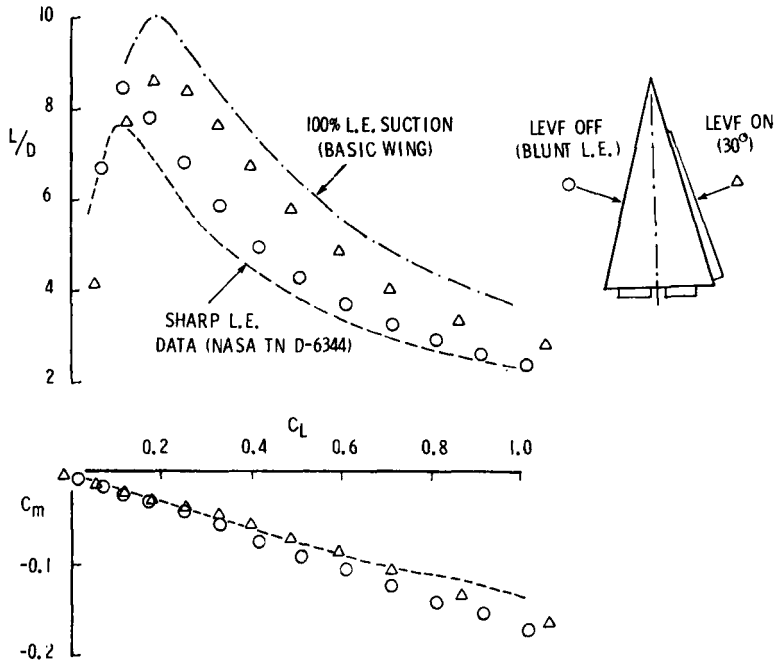

Figure 2.- Vortex-flap test results on 74° delta wing.

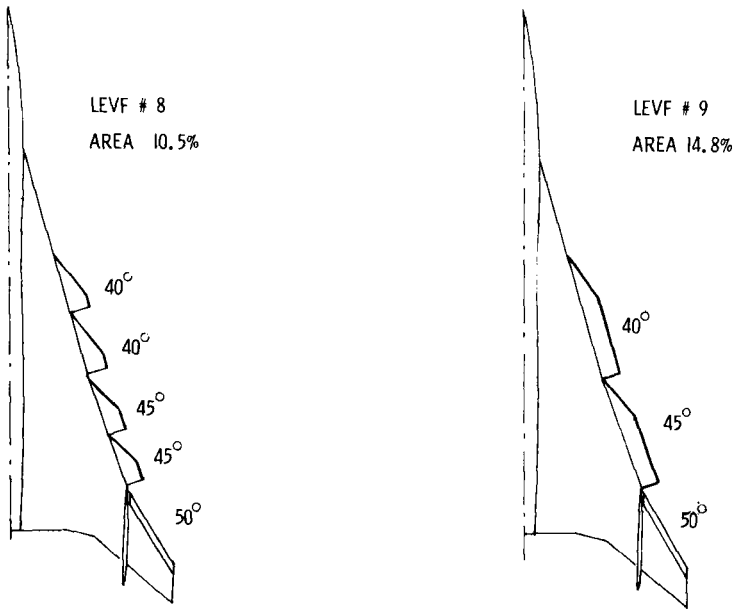

Figure 3.- Vortex-flap configurations on SWAT model.

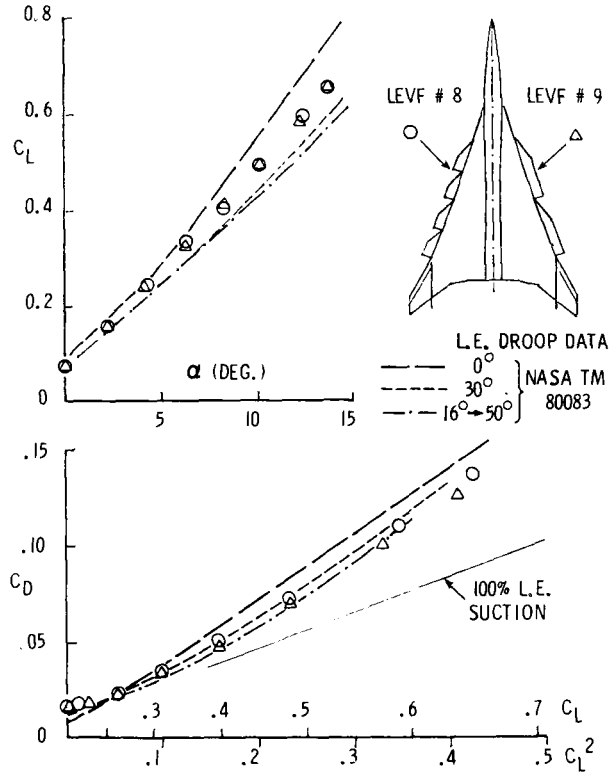

Figure 4.- Lift and drag comparison of vortex-flaps with leading-edge droop.

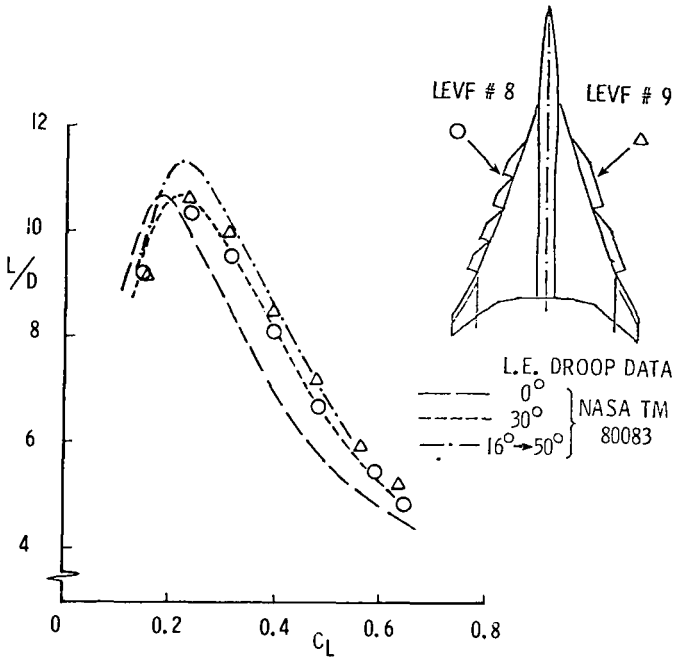

Figure 5.- Lift/drag ratio comparison of vortex-flaps with leading-edge droop.

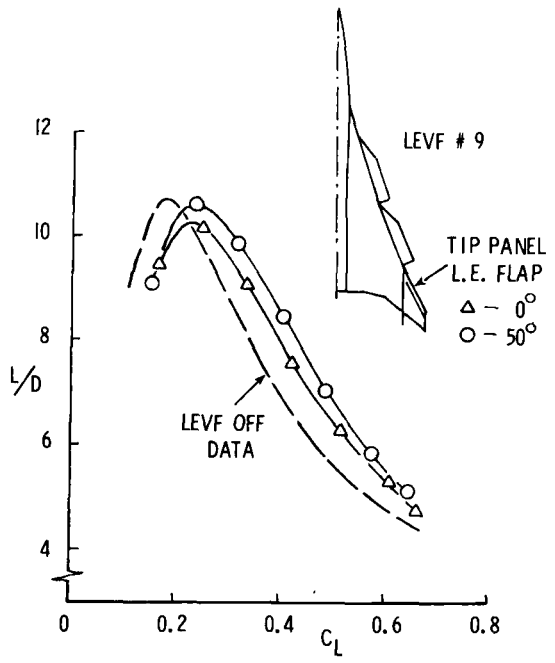

Figure 6.- Effect of tip-panel leading-edge flap deflection on lift/drag ratio.

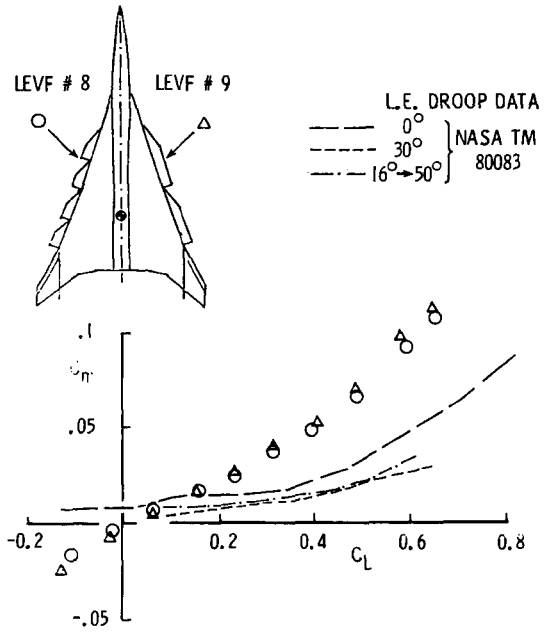

Figure 7.- Pitching moment comparison of vortex-flaps with leading edge droop.

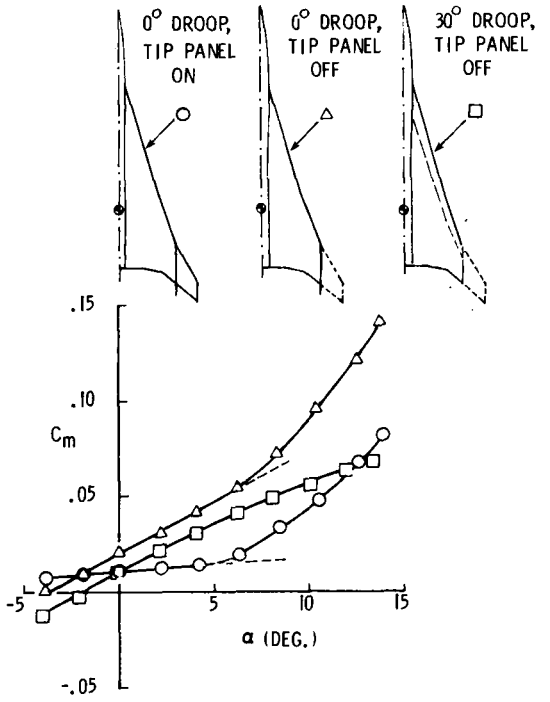

Figure 8.- Effects of leading-edge droop and tip panel on pitch-up.

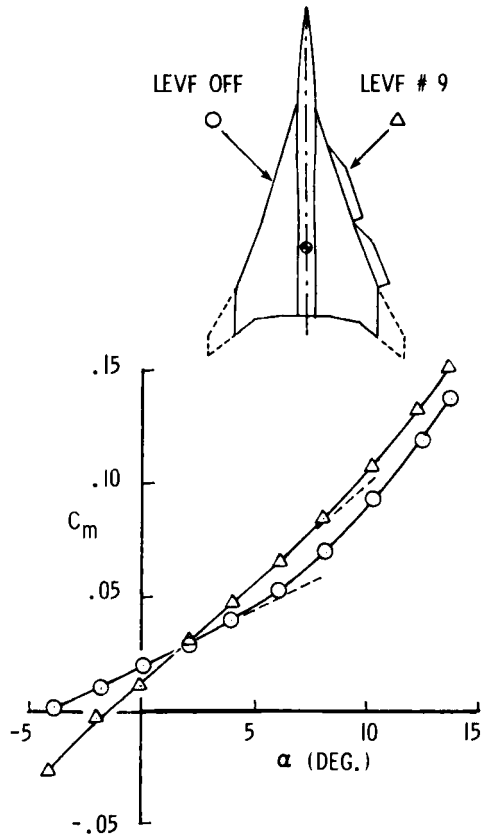

Figure 9.- Vortex-flap effect on longitudinal stability (tip-panels off).

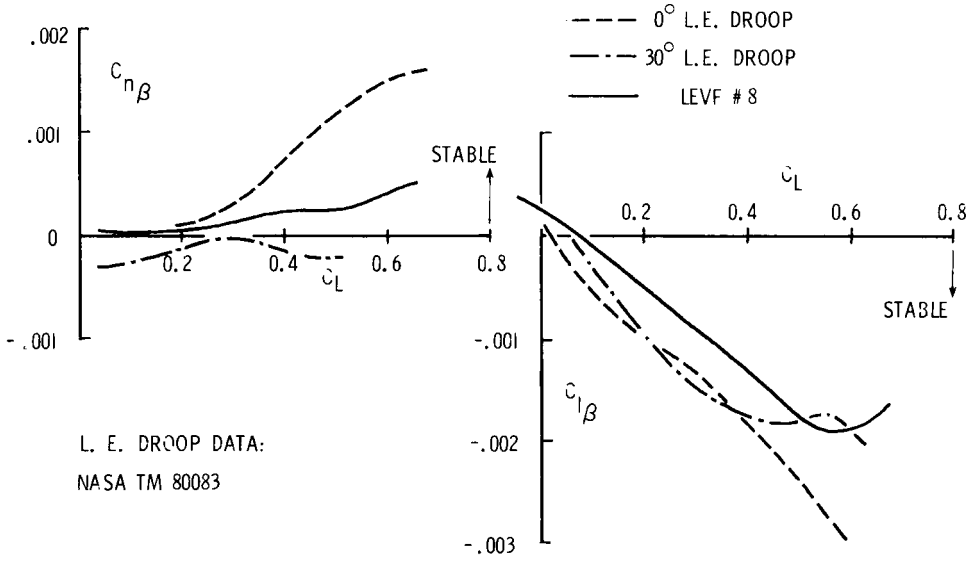

Figure 10.- Vortex-flap effects on directional and lateral stability.

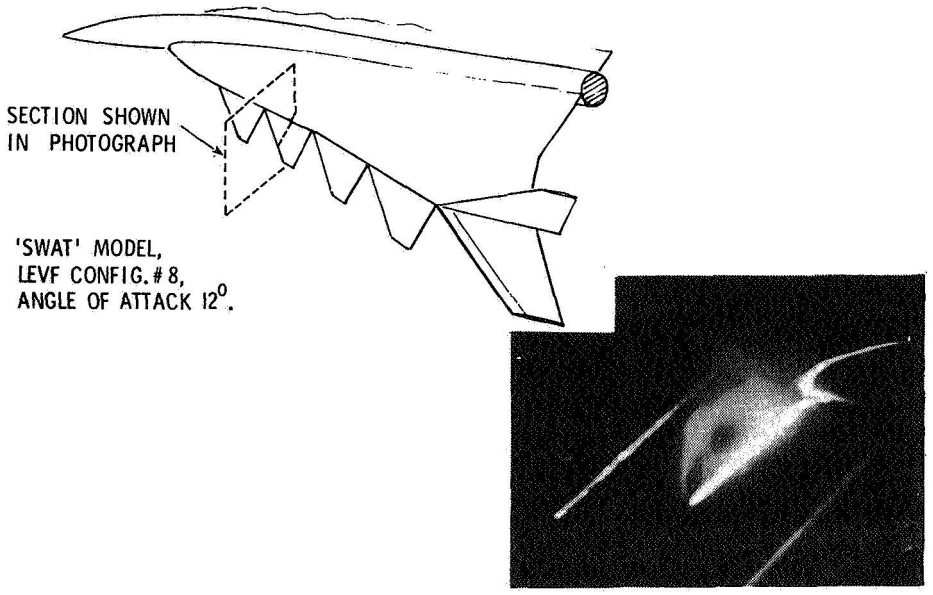

Figure 11.- Smoke flow visualization on vortex-flap.